

A Comparison between RSMA, SDMA, and OMA in Multibeam LEO Satellite Systems

Alea Schröder*, Maik Röper*, Dirk Wübben*, Bho Matthiesen^{*†}, Petar Popovski^{‡,†} and Armin Dekorsy*

* Gauss-Olbers Center, c/o University of Bremen, Dept. of Communications Engineering, 28359 Bremen, Germany

† University of Bremen, U Bremen Excellence Chair, Dept. of Communications Engineering, 28359 Bremen, Germany

‡ Aalborg University, Department of Electronic Systems, 9220 Aalborg, Denmark

Email: {schroeder,roeper,wuebben,matthiesen,dekorsy}@ant.uni-bremen.de, petarp@es.aau.dk

Abstract

Low Earth orbit (LEO) satellite systems enable close to global coverage and are therefore expected to become important pillars of future communication standards. However, a particular challenge faced by LEO satellites is the high orbital velocities due to which a precise channel estimation is difficult. We model this influence as an erroneous angle of departure (AoD), which corresponds to imperfect channel state information (CSI) at the transmitter (CSIT). Poor CSIT and non-orthogonal user channels degrade the performance of space-division multiple access (SDMA) precoding by increasing inter-user interference (IUI). In contrast to SDMA, there is no IUI in orthogonal multiple access (OMA), but it requires orthogonal time or frequency resources for each user. Rate-splitting multiple access (RSMA), unifying SDMA, OMA, and non-orthogonal multiple access (NOMA), has recently been proven to be a flexible approach for robust interference management considering imperfect CSIT. In this paper, we investigate RSMA as a promising strategy to manage IUI in LEO satellite downlink systems caused by non-orthogonal user channels as well as imperfect CSIT. We evaluate the optimal configuration of RSMA depending on the geometrical constellation between the satellite and users.

Index Terms

Low Earth orbit (LEO), Rate-Splitting Multiple Access, multi-user beamforming, MIMO satellite communications, beamspace MIMO, angle division multiple access, 3D networks

I. INTRODUCTION

Mobile networks are currently evolving from being focused on low-altitude and ground-based devices towards three-dimensional (3D) networks. Incorporating air- and spaceborne terminals into the sixth generation (6G) of mobile networks is expected to lead to ubiquitous global connectivity, a reduced carbon footprint of information

This article is presented in part at the 2023 International ITG 26th Workshop on Smart Antennas and 13th Conference on Systems, Communications, and Coding.

and communication technology, and much higher resilience of the terrestrial network infrastructure. An integral step towards this goal is the integration of non-terrestrial networks (NTN) into the current infrastructure [1]–[3]. In particular, low Earth orbit (LEO) satellites have gained a lot of interest due to their significantly reduced latency, path losses, and deployment costs compared to conventional high-throughput satellites in medium Earth orbit (MEO) and geostationary orbit (GEO) [2], [4]. However, the low altitude of 500–2000 km causes high velocities relative to terrestrial components. This is introducing a host of challenges including high Doppler shifts and imperfect channel state estimation due to imprecise position measurement. These obstacles challenge conventional multiple access schemes like orthogonal multiple access (OMA) and space-division multiple access (SDMA). The common OMA scheme since the fourth generation of mobile networks is to assign orthogonal time or frequency resources for each user, i.e., a combination of orthogonal frequency-division multiple access (OFDMA) and time-division multiple access (TDMA) [5]. However, OFDMA is highly sensitive to Doppler shifts, while TDMA becomes very challenging for large and time-varying transmission delays [5]. On the other hand, SDMA enables higher spectral efficiencies compared to OMA but it requires multi-user precoding based on recent channel state information (CSI) in order to mitigate the mutual inter-user interference (IUI) [6]. The effectiveness of the precoder, and correspondingly the mutual IUI, depends on the spatial separation of the users and the accuracy of the CSI at the transmitter (CSIT). High delays and relative velocities to the users on the ground impede the acquisition of CSI at the satellites.

A promising multiple access scheme in case of erroneous CSIT is called rate-splitting multiple access (RSMA). While unifying SDMA, OMA, and non-orthogonal multiple access (NOMA) [7], RSMA has been shown to flexibly manage IUI for a wide range of applications [8]. In RSMA, each user message is split into a private and a common part. The common part messages of all users are jointly encoded into a common data stream for all users. Depending on the amount of correlation between the user channels and errors of imperfections, different amounts of power are assigned to the common and private parts. Originally, RSMA has been investigated for use in terrestrial networks [9] but has recently been extended to satellite use cases in [10], [11], among others. While investigation for terrestrial communications such as [9], [12] tend to assume a Rayleigh fading channel, satellite communication is better covered by line-of-sight (LOS) channel models [4], [13]. In [7], the authors investigated RSMA for different amounts of correlation between the user channels in a two-user scenario for LOS and Rayleigh fading channels considering perfect CSIT. Our work complements their research by expanding their setting to a LEO satellite downlink scenario. We, therefore, consider a LOS channel model and introduce an erroneous angle of departure (AoD) to model imperfect position knowledge at the satellite. Furthermore, we study the optimal power allocation between common and private parts in RSMA depending on the level of correlation between the user channels while considering imperfect position knowledge. We compare the corresponding RSMA performance to OMA and SDMA. Our results show that RSMA outperforms both schemes by flexibly managing the IUI.

The paper is organized as follows. Section II presents the LEO downlink satellite system model as well as the conventional multiple access schemes, SDMA and OMA. Section III introduces the RSMA approach, which is numerically evaluated in section IV. The results are concluded and discussed in Section V.

Notation: Lower and upper boldface letters denote vectors \mathbf{x} and matrices \mathbf{X} , respectively. $\{\cdot\}^T$, $\{\cdot\}^H$ are indicating the transpose and complex conjugate transpose operator, while \circ is the Hadamard product. The Euclidean norm is

given by $\|\cdot\|$, absolute values by $|\cdot|$.

II. SYSTEM MODEL

A. LOS Channel

In this section, we introduce the LEO downlink LOS system model as well as the assumed phase error model for imperfect CSIT. One LEO satellite, equipped with a uniform linear array (ULA) containing N antennas, serves K users. The users are handheld devices equipped with a single antenna with low receive gain G_{user} . For the transmission from the satellite to user k , we assume a LOS channel vector $\mathbf{h}_k \in \mathbb{C}^{1 \times N}$ and complex additive white Gaussian noise (AWGN) $n_k \sim \mathcal{CN}(0, \sigma_n^2)$. The received signal y_k for a given signal vector \mathbf{x} and user k is described by

$$y_k = \sum_{n=1}^N \mathbf{h}_{k,n} \mathbf{x}_n + n_k, \quad (1)$$

where $\mathbf{x} \in \mathbb{C}^{N \times 1}$ is the linearly precoded signal vector, which differs depending on the chosen multiple access scheme and precoder design.

For LEO satellites the transmission is mainly characterized by the LOS channel component. A corresponding channel vector \mathbf{h}_k for the k -th user is given by [14]

$$\mathbf{h}_k(\cos(\theta_k)) = \sqrt{G_{\text{user}} G_{\text{sat}}} \frac{\lambda}{4\pi d_k} \mathbf{e}^{-j\varphi_k} \mathbf{a}_k^T(\cos(\theta_k)), \quad (2)$$

where G_{sat} is the satellite antenna gain, λ the wavelength and d_k the distance from the satellite to user k . The overall phase shift of the symbols from the satellite to user k is determined by $\varphi_k \in [0, 2\pi]$. The relative phase shifts between the N satellite antennas towards user k are described by the steering vector $\mathbf{a}_k(\cos(\theta_k)) = [a_k^1(\cos(\theta_k)), \dots, a_k^N(\cos(\theta_k))]^T$, where θ_k is the AoD from the ULA origin to user k . Fig. 1 shows the AoDs θ_k and θ_{k-1} of two users k and $k-1$ in a LEO satellite downlink scenario with a satellite altitude d_0 and user distance D_k . In general, the n -th element of the steering vector $\mathbf{a}_k(\eta_k)$ for user k with a given argument $\eta_k = \cos(\theta_k)$ is given as

$$a_k^n(\eta_k) = \exp^{-j\pi \frac{d_N}{\lambda} (N+1-2n)\eta_k} \quad (3)$$

where d_N denotes the distance between the satellite antenna elements.

Due to the high velocity of LEO satellites, a precise estimation of the user positions might not be available at the satellite. The channel vector $\mathbf{h}_k(\cos(\theta_k))$ of user k with the steering vector $\mathbf{a}_k(\cos(\theta_k))$ is highly dependent on the AoD θ_k of user k . In particular, the relative phase shifts between the satellite antenna elements, which determine the performance of SDMA precoding, are characterized by the AoDs of the users [15]. We, therefore, model imprecise position measurement as an erroneous AoD. Instead of adding an error directly on the AoD θ_k , we consider an additive error on the $\cos(\theta_k)$. This error is a uniformly distributed additive error $\varepsilon_k \sim \mathcal{U}(-\Delta\varepsilon, +\Delta\varepsilon)$,

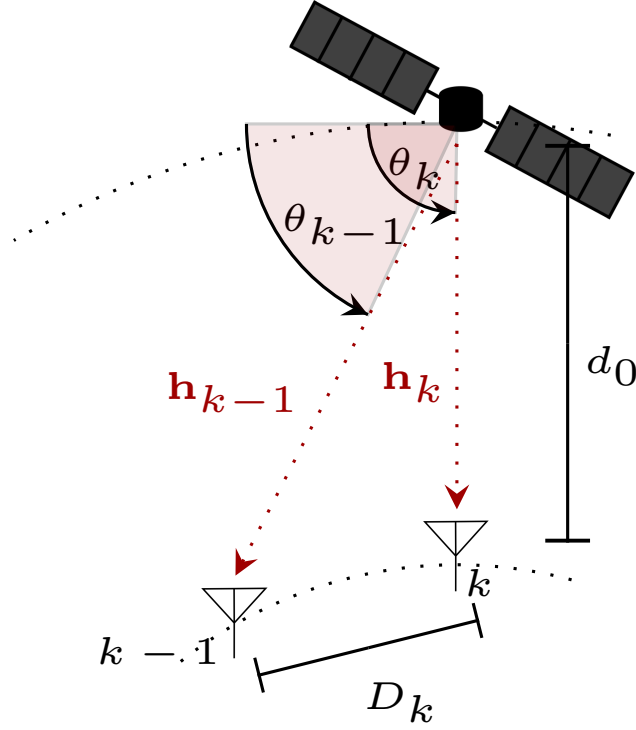


Fig. 1. Single satellite scenario with a satellite altitude d_0 and two users k and $k-1$, positioned at the AoDs θ_k and θ_{k-1} , characterized by the channel vectors \mathbf{h}_k and \mathbf{h}_{k-1} and their distance D_k .

that follows the same distribution for all user k . Therefore, and by using the definition of the steering vector (3), we can interpret the additive phase error ε_k as an overall multiplicative error $\mathbf{a}_k(\varepsilon_k)$ on the channel vector \mathbf{h}_k . Then, the estimated channel vector $\tilde{\mathbf{h}}_k$ can be written as

$$\tilde{\mathbf{h}}_k(\cos(\theta_k)) = \mathbf{h}_k(\cos(\theta_k)) \circ \mathbf{a}_k^T(\varepsilon_k). \quad (4)$$

The precoding will be based on this channel estimation $\tilde{\mathbf{h}}_k$. In the following subsections, we introduce the multiple access schemes SDMA and OMA.

B. Space-division multiple access (SDMA)

In SDMA, the user messages are spatially separated by beams that ideally steer a maximum amount of power into the user directions while minimizing the interference between the beams. Therefore, each user symbol s_k is weighted by a precoding vector \mathbf{w}_k . Because the K users share the same time and frequency resources, the signal vector \mathbf{x} is given as a superposition of all weighted user symbols

$$\mathbf{x} = \sum_{k=1}^K \mathbf{w}_k s_k. \quad (5)$$

We analyze the performance of the different precoding strategies by evaluating their corresponding sum rate R , which is determined by the signal-to-interference-and-noise ratio (SINR) of each user k . Assuming Gaussian distributed transmit symbols, the sum rate is generally formulated as [16],

$$R^{\text{SDMA}} = \sum_{k=1}^K \log \left(1 + \frac{|\mathbf{h}_k \mathbf{w}_k|^2}{\sigma_n^2 + \sum_{i \neq k} |\mathbf{h}_k \mathbf{w}_i|^2} \right). \quad (6)$$

In Section III we extend this formulation to the RSMA method.

The minimum mean-squared error (MMSE) precoder is a well-established and reliable SDMA precoder [17], [18]. A corresponding precoding matrix $\mathbf{W} = [\mathbf{w}_1 \dots \mathbf{w}_K]$ is specified as

$$\begin{aligned} \mathbf{W} &= \sqrt{\frac{P}{\text{tr}\{\mathbf{W}'^H \mathbf{W}'\}}} \cdot \mathbf{W}' \\ \mathbf{W}' &= \left[\tilde{\mathbf{H}}^H \tilde{\mathbf{H}} + \sigma_n^2 \cdot \frac{K}{P} \cdot \mathbf{I}_N \right]^{-1} \tilde{\mathbf{H}}^H \end{aligned} \quad (7)$$

where $\tilde{\mathbf{H}} = [\tilde{\mathbf{h}}_1 \dots \tilde{\mathbf{h}}_K]^T$ is the complete estimated channel matrix according to (4). Corresponding to this definition of the MMSE precoder, the transmit power P is not always equally distributed among the K users. In particular, the transmit power of a user k with a bad channel, i.e., \mathbf{h}_k has a small euclidean norm, is higher than for those with good channels. This behavior introduces some fairness among the different users but does not maximize the corresponding sum rate (6).

C. Orthogonal multiple access (OMA)

To not only evaluate the RSMA approach in comparison with SDMA precoding, we compare both approaches to an OMA approach. In OMA, all users receive their symbols via orthogonal time or frequency resources, such that there is no IUI on the received signals. In this case, the precoding approach maximizing the rate of user k is maximum ratio transmission (MRT). It steers the maximum amount of the available transmit power per user into its direction. With equal power allocation among the users, this precoder is given by

$$\mathbf{w}_k^{\text{MRT}} = \sqrt{\frac{P}{K}} \cdot \frac{\tilde{\mathbf{h}}_k^H}{\|\tilde{\mathbf{h}}_k\|}. \quad (8)$$

In contrast to the SDMA approach, each user is only assigned to $1/K$ th time or frequency resources, which limits the corresponding rate. Thus, the sum rate for OMA becomes

$$R^{\text{OMA}} = \frac{1}{K} \sum_{k=1}^K \log \left(1 + \frac{|\mathbf{h}_k \mathbf{w}_k|^2}{\sigma_n^2} \right). \quad (9)$$

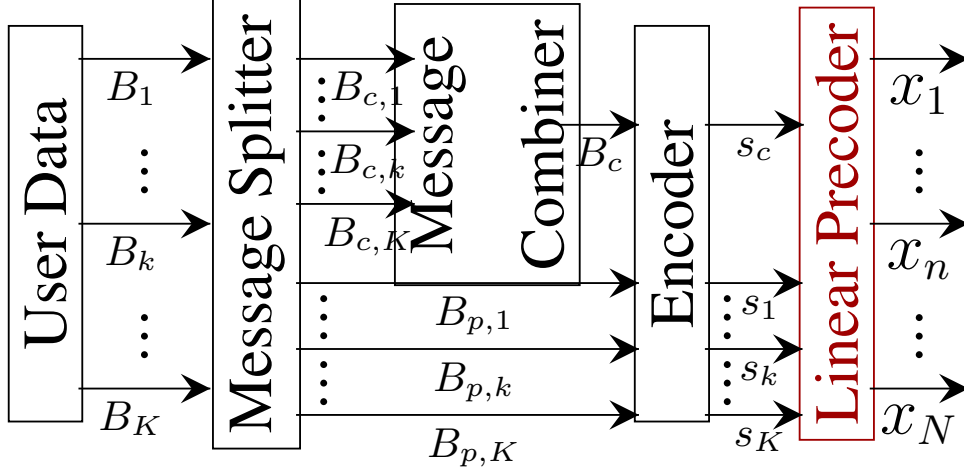


Fig. 2. Process Flow Diagram of RSMA. User data is split into a private and a common part. All common parts are combined into one message, which is destined for all users.

Note that the common OMA approaches OFDMA and TDMA are highly sensitive to the high Doppler shifts and delays of LEO satellite communication systems [5]. In this paper, we neglect these influences on the transmission quality by assuming a perfect compensation of the effects.

Next, we introduce the RSMA approach and define an achievable rate, similar to the sum rate, as the corresponding evaluation metric.

III. RATE-SPLITTING MULTIPLE ACCESS

To perform RSMA each user message B_k is split into a private part $B_{p,k}$ and a common part $B_{c,k}$. Fig. 2 presents a corresponding process flow diagram. In the following, the index p marks private part entities, whereas c indicates the common part. After splitting each user's message into a private and a common part, the common part messages $B_{c,k}$ of all K users are combined into one common part message B_c . All private part messages $\{B_{p,k}\}_{k=1}^K$ and the common part message B_c is encoded into symbols, such that each user is assigned one private symbol s_k and the common symbol s_c . These symbols are precoded linearly and the resulting transmit vector $\mathbf{x} \in \mathbb{C}^{N \times 1}$ follows as [8],

$$\mathbf{x} = \mathbf{w}_c s_c + \sum_{k=1}^K \mathbf{w}_{p,k} s_k, \quad (10)$$

where $\mathbf{w}_c \in \mathbb{C}^{N \times 1}$ is the common part precoding vector and $\mathbf{w}_{p,k} \in \mathbb{C}^{N \times 1}$ is the private part precoding vector of user k . The design of these precoding vectors is pursued in the subsequent subsection, followed by the generalization of the sum rate for the RSMA case.

A. Precoder Design

An important design criterion in RSMA is the optimal allocation of total transmit power P to the precoding vectors of the private parts $\mathbf{w}_{p,k}$ and the common part precoding vector \mathbf{w}_c . Therefore, a scaling factor $\alpha \in [0, 1]$ is introduced, such that the power allocation among the precoding vectors is given by

$$\begin{aligned} \|\mathbf{w}_c\|^2 &= P - P^\alpha \\ \sum_{k=1}^K \|\mathbf{w}_{p,k}\|^2 &= P^\alpha. \end{aligned} \quad (11)$$

A scaling factor of $\alpha = 1$ equals common SDMA precoding, whereas a theoretical factor of $\alpha \rightarrow -\infty$ would correspond to multicast transmission. In order to directly examine the influence of the scaling factor α on the RSMA performance, we assume the same precoding methods for any given channel realization. For the common part precoding vector \mathbf{w}_c , we choose a basic precoder that is independent of any CSIT,

$$\mathbf{w}_c = \sqrt{\frac{P - P^\alpha}{N}} \cdot [1 \dots 1]^T. \quad (12)$$

Whereas we apply MMSE precoding according to (7) for the private part precoding. In order to fulfill the power constraints from (11), the transmit power P is reduced to P^α , such that the private part precoding matrix \mathbf{W}_p follows as

$$\begin{aligned} \mathbf{W}_p &= \sqrt{\frac{P^\alpha}{\text{tr}\{\mathbf{W}'^H \mathbf{W}'\}}} \cdot \mathbf{W}' \\ \mathbf{W}' &= \left[\tilde{\mathbf{H}}^H \tilde{\mathbf{H}} + \sigma_n^2 \cdot \frac{K}{P^\alpha} \cdot \mathbf{I}_N \right]^{-1} \tilde{\mathbf{H}}^H \end{aligned} \quad (13)$$

B. Achievable Rate

To evaluate the performance of RSMA, we need to extend the sum rate metric to the common part. With the signal vector $\mathbf{x} \in \mathbb{C}^{N \times 1}$ from (10) and (1), the receive signal y_k is given by

$$y_k = \mathbf{h}_k \mathbf{w}_c s_c + \mathbf{h}_k \mathbf{w}_{p,k} s_k + \mathbf{h}_k \sum_{i \neq k} \mathbf{w}_{p,i} s_i + n_k. \quad (14)$$

In RSMA, the common part symbol s_c is the first to be decoded by successive interference cancellation (SIC). This requires additional receiver complexity compared to SDMA precoding [8]. For perfect SIC, the rate for the common part symbol $R_{c,k}$ of user k is given by

$$R_{c,k} = \log \left(1 + \frac{|\mathbf{h}_k \mathbf{w}_c|^2}{\sigma_n^2 + \sum_{i=1}^K |\mathbf{h}_k \mathbf{w}_{p,i}|^2} \right), \quad (15)$$

that takes the interference of all private parts into account. The remaining received signal after the successful decoding of the common part is

$$y_{p,k} = \mathbf{h}_k \mathbf{w}_{p,k} s_k + \mathbf{h}_k \sum_{i \neq k} \mathbf{w}_{p,i} s_i + n_k. \quad (16)$$

For the residual signal $y_{p,k}$, the IUI will be treated as noise, such that the corresponding private rate $R_{p,k}$ of user k results in

$$R_{p,k} = \log \left(1 + \frac{|\mathbf{h}_k \mathbf{w}_{p,k}|^2}{\sigma_n^2 + \sum_{i \neq k}^K |\mathbf{h}_k \mathbf{w}_{p,i}|^2} \right). \quad (17)$$

To get an equivalent rate compared to (6), all private part rates are summed up, and the smallest common part rate is added to guarantee successful common part decoding at all users [8]. The specific sum rate for RSMA precoding calculates as

$$R^{\text{RSMA}} = \min_k R_{c,k} + \sum_{k=1}^K R_{p,k}. \quad (18)$$

Note that in this paper, we assume simple common part precoding (12) and MMSE private part precoding (13). We do not follow an optimal design based on (18).

IV. NUMERICAL EVALUATIONS

In this paper, we investigate RSMA for a LOS channel with multiplicative error (4). Given that RSMA was originally designed for Rayleigh fading channels with additive errors, our goal is to evaluate its suitability for robust interference management in LEO satellite downlink scenarios. All numerical evaluations in this section consider a two-user downlink scenario and the simulation parameters from Table I. This section is organized as follows. In Section IV-A we evaluate SDMA and RSMA for different realizations of the deterministic LOS channel (2) assuming perfect CSIT. In Section IV-B we expand this evaluation to a scenario with imperfect CSIT, e.g., an error on the AoDs according to (4).

A. Perfect CSIT

The LOS channel characteristics, as defined in Section II-A, highly differ depending on the given satellite altitude d_0 , the number of transmit antennas N , their inter-antenna-distance d_N , and the AoDs of the users. In this paper, we solely focus on the impact of the AoDs on the channel characteristics. The AoD θ_1 , see Fig. 1, from the satellite to the first user is 90° . User 1, therefore, is positioned directly underneath the satellite with the smallest satellite-to-user distance $d_1 = d_0 = 600$ km. Whereas the position of user 2, e.g., the AoD θ_2 , is variable. The difference $\Delta\theta$ between the AoD θ_2 of user 2 and the AoD θ_1 of user 1 is assigned to a corresponding user distance D_k . Depending on this difference $\Delta\theta$ and therefore depending on the user distance D_k , the characteristics of the LOS channel vary.

TABLE I
SIMULATION PARAMETER

User Number	K	2
Satellite altitude	d_0	600 km
Carrier frequency	f	2 GHz
Satellite antenna number	N	6
Inter-antenna-spacing	d_N	7.5 cm
Satellite antenna gain	G_{sat}	16 dBi
User antenna gain	G_{user}	0 dBi
Noise Power	σ_n^2	-122 dBW
Transmit Power	P	20 dBW

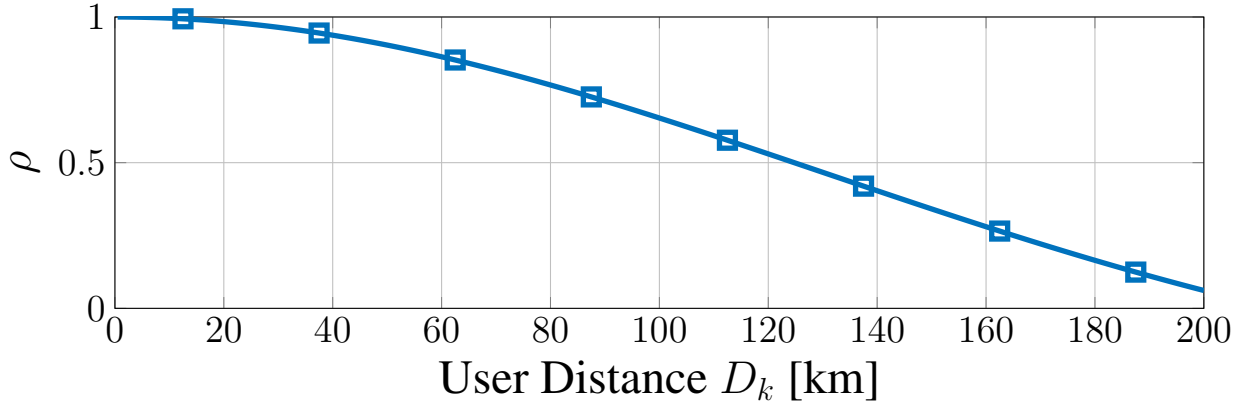


Fig. 3. Correlation factor ρ depending on the User Distance D_k

We introduce a correlation factor ρ to quantify the amount of correlation between the channel vectors of both users,

$$\rho = \frac{\mathbf{h}_1^H \mathbf{h}_2}{\|\mathbf{h}_1\| \|\mathbf{h}_2\|}. \quad (19)$$

Accordingly, a correlation factor $\rho = 1$ corresponds to aligned channels, while a correlation factor $\rho = 0$ corresponds to orthogonal channels. Fig. 3 shows how the amount of correlation ρ between the user channels decreases with an increasing user distance D_k for $D_k \leq 200$ km.

Fig. 4 depicts the achievable rates of SDMA, OMA, and RSMA for user distances D_k between 0.5 km and 200 km. SDMA precoding performs best for orthogonal user channels. The higher the correlation factor ρ , the higher the IUI, which cannot be compensated by common SDMA precoding. To manage this mutual IUI, we apply RSMA. The RSMA approach is shown for different power scaling factors α . The larger α the more power is assigned to the private parts, i.e. a scaling factor $\alpha = 1$ equals SDMA precoding. RSMA opt. refers to an optimal

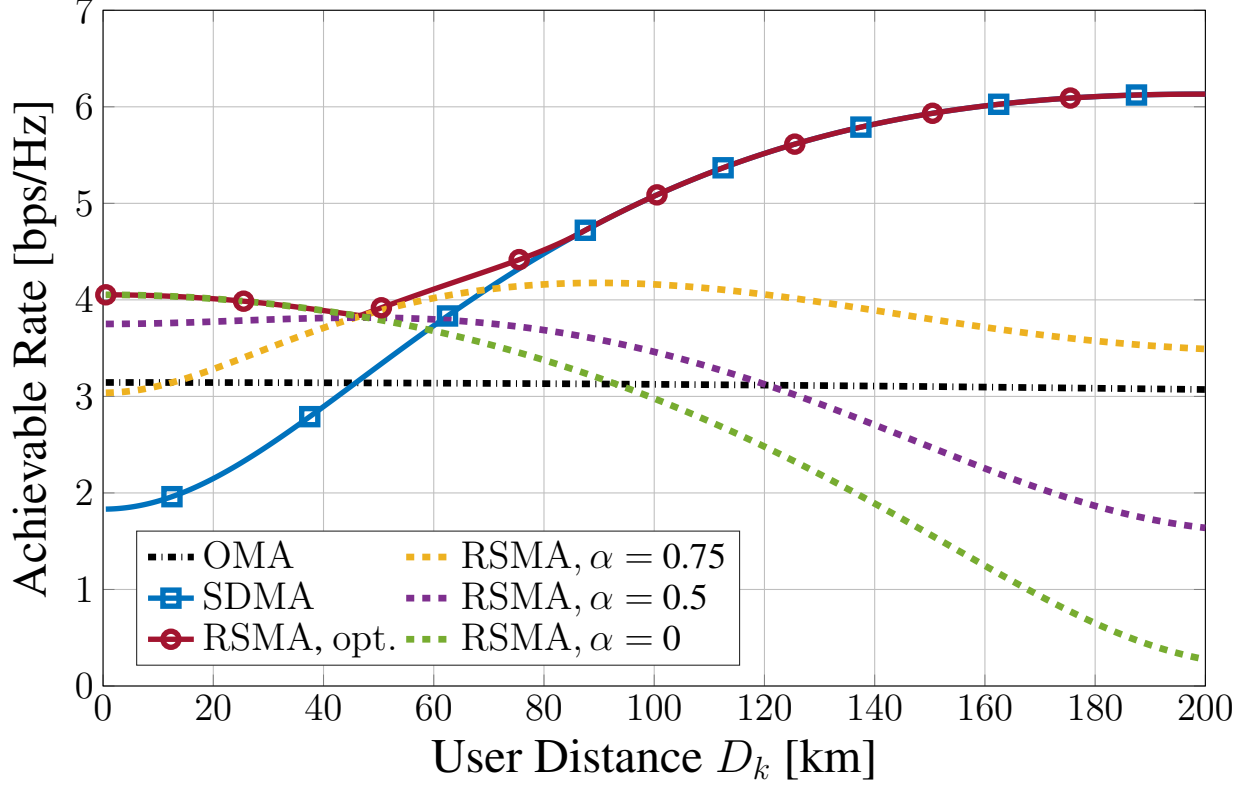


Fig. 4. Comparison of Achievable Rates between SDMA, OMA and different realizations of RSMA depending on the User Distance D_k for perfect CSIT. RSMA, opt. corresponds to the optimal scaling factor α_{opt} for any given User Distance D_k .

α_{opt} for each user distance D_k and is obtained by exhaustive search. RSMA opt. outperforms the OMA approach for all values of D_k . Further, it is showing strong performance gains compared to SDMA for user distances D_k up to roughly 80 km. For larger user distances RSMA opt. and SDMA attain the same achievable rate. Therefore, the optimal α for $D_k > 80$ km is $\alpha_{\text{opt}}|_{D_k > 80 \text{ km}} = 1$. For user distances D_k smaller than 48 km, which corresponds to the intersection between SDMA and OMA, RSMA opt. follows the line of RSMA for $\alpha = 0$. It can be observed that the performance of RSMA for $\alpha = 0$ and therefore the performance of RSMA opt. slightly decreases in this area with increasing user distance D_k . This is due to the likewise decreasing correlation between the user channels, which is favorable for the transmission of the private parts but disadvantageous for the transmission of the common part, which is intended for all users. For $\alpha = 0$ and an overall transmit power of $P = 20$ dBW 99% of the transmit power is assigned to the common part. Whereas there is no transmit power in the common part for $\alpha = 1$. Only for user distances D_k between 48 km and 80 km scaling factors other than zero or one achieve the optimal RSMA performance for the given precoder designs. In general, it can be concluded that the higher the correlation between the channels, the smaller the optimal scaling factor α_{opt} and vice versa.

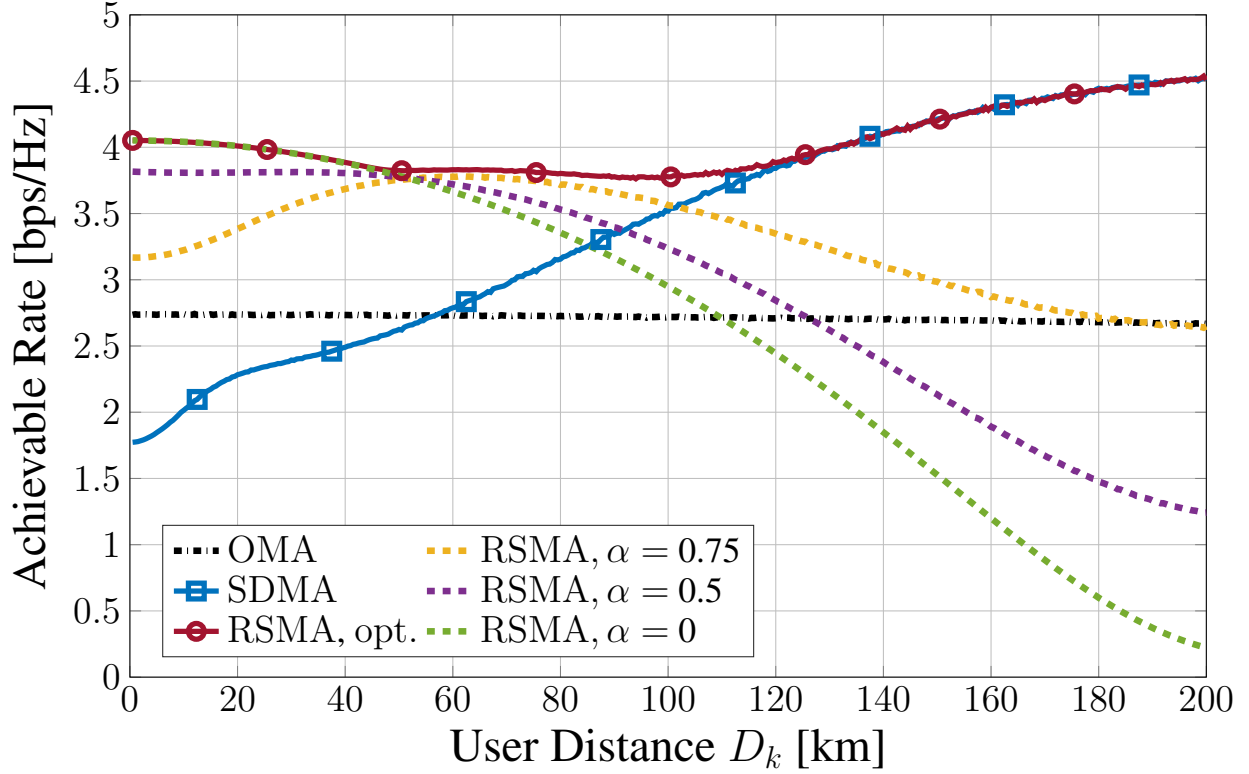


Fig. 5. Comparison of Achievable Rates between SDMA, OMA and different realizations of RSMA depending on the User Distance D_k for imperfect CSIT, e.g., an uniformly distributed additive error $\varepsilon = 0.2$ on the cosine of the AoDs of both users. RSMA, opt. corresponds to the optimal scaling factor α_{opt} for any given User Distance D_k .

B. Imperfect CSIT

To expand the evaluation of RSMA in LEO satellite downlink scenarios, we now consider a scenario with imperfect CSIT. Therefore, a uniformly distributed error ε_k with $\Delta\varepsilon = 0.2$ (see Section II-A) is applied on the cosine of the AoDs of the users. It can be interpreted as uncertainty in the user positions. Fig. 5 shows the corresponding achievable rates for SDMA, OMA, and RSMA averaged over 10 000 Monte Carlo iterations. As expected the performance of common SDMA precoding is reduced compared to the scenario with perfect CSIT. The maximum achievable rate, for example, dropped from 6.1 bps/Hz to 4.5 bps/Hz for a user distance of $D_k = 200$ km. Further, in the perfect CSIT scenario SDMA outperformed OMA for user distances D_k larger than roughly 48 km, whereas the intersection point for the imperfect CSIT scenario is at approximately 58 km. Note that the achievable rate for OMA is also decreased by 13 % to 2.7 bps/Hz compared to the perfect CSIT scenario. In contrast to that, RSMA opt. is able to maintain a rate of at least 3.8 bps/Hz over the complete interval of D_k . Though the maximum achievable rate for $D_k = 200$ km of the perfect CSIT case is not obtained, RSMA opt. still outperforms common SDMA for user distances up to 120 km compared to 80 km in the perfect CSIT scenario. The area in which RSMA prevails over common SDMA precoding is therefore increased by imperfect CSIT.

V. CONCLUSION AND DISCUSSION

In this paper, RSMA was applied in a LEO satellite downlink scenario with a LOS channel and a multiplicative error on the channel vector. For the precoding of the common and the private parts, we implemented well-known and feasible precoding strategies. It was shown that RSMA is able to flexibly manage IUI for correlated user channels and imperfect CSIT by adapting its power scaling factor to the given channel realization. It thereby prevails common SDMA precoding. In practice, of course, the optimal scaling factor can not be found by exhaustive search for every channel realization. Therefore, further study is required on how to utilize RSMA in satellite communication scenarios.

ACKNOWLEDGMENT

This research was supported in part by the German Federal Ministry of Education and Research (BMBF) within the project Open6GHub under grant number 16KISK016 and by the German Research Foundation (DFG) under Germany's Excellence Strategy (EXC 2077 at University of Bremen, University Allowance).

REFERENCES

- [1] 3GPP TR 38.863, "Technical specification group radio access network; solutions for nr to support non-terrestrial networks (NTN): Non-terrestrial networks (NTN) related RF and co-existence aspects (release 17)," Sep. 2022.
- [2] I. Leyva-Mayorga, B. Soret, M. Röper, D. Wübben, B. Matthiesen, A. Dekorsy, and P. Popovski, "LEO small-satellite constellations for 5G and beyond-5G communications," *IEEE Access*, vol. 8, pp. 184 955–184 964, 2020.
- [3] Z. Qu, G. Zhang, H. Cao, and J. Xie, "LEO Satellite Constellation for Internet of Things," *IEEE Access*, vol. 5, pp. 18 391–18 401, 2017.
- [4] M. Röper, B. Matthiesen, D. Wübben, P. Popovski, and A. Dekorsy, "Beam-space MIMO for Satellite Swarms," in *Proc. IEEE Wireless Commun. Netw. Conf. (WCNC)*, 2022, pp. 1307–1312.
- [5] A. Guidotti *et al.*, "Architectures and key technical challenges for 5G systems incorporating satellites," *IEEE Trans. Veh. Technol.*, vol. 68, no. 3, pp. 2624–2639, Mar. 2019.
- [6] P. Vandenameele, L. Van Der Perre, M. Engels, B. Gyselinckx, and H. De Man, "A combined OFDM/SDMA approach," *IEEE Journal on Selected Areas in Communications*, vol. 18, no. 11, pp. 2312–2321, 2000.
- [7] B. Clerckx, Y. Mao, R. Schober, and H. V. Poor, "Rate-splitting unifying SDMA, OMA, NOMA, and multicasting in MISO broadcast channel: A simple two-user rate analysis," *IEEE Wireless Communication Letters*, vol. 9, no. 3, pp. 349–353, 2020.
- [8] Y. Mao, O. Dizdar, B. Clerckx, R. Schober, P. Popovski, and H. V. Poor, "Rate-splitting multiple access: Fundamentals, survey, and future research trends," *IEEE Communications Surveys & Tutorials*, 2022.
- [9] M. Dai, B. Clerckx, D. Gesbert, and G. Caire, "A rate splitting strategy for massive MIMO with imperfect CSIT," *IEEE Transactions on Wireless Communications*, vol. 15, no. 7, pp. 4611–4624, 2016.
- [10] L. Yin and B. Clerckx, "Rate-Splitting Multiple Access for Satellite-Terrestrial Integrated Networks: Benefits of Coordination and Cooperation," *IEEE Transactions on Wireless Communications*, 2022.
- [11] M. Vazquez, M. Caus, and A. Perez-Neira, "Rate splitting for MIMO multibeam satellite systems," in *Proceeding of 22nd International ITG Workshop on Smart Antennas (WSA)*, 2018.
- [12] J. Choi, N. Lee, S.-N. Hong, and G. Caire, "Joint user selection, power allocation, and precoding design with imperfect CSIT for multi-cell MU-MIMO downlink systems," *IEEE Transactions on Wireless Communications*, vol. 19, no. 1, pp. 162–176, 2020.
- [13] R. T. Schwarz, T. Delamotte, K.-U. Storek, and A. Knopp, "MIMO applications for multibeam satellites," *IEEE Transactions on Broadcasting*, vol. 65, no. 4, pp. 664–681, 2019.
- [14] L. You, K. X. Li, J. Wang, X. Gao, X. G. Xia, and B. Ottersten, "Massive MIMO transmission for LEO satellite communications," *IEEE J. Sel. Areas Commun.*, vol. 38, no. 8, pp. 1851–1865, 2020.
- [15] M. Röper, B. Matthiesen, D. Wübben, P. Popovski, and A. Dekorsy, "Distributed downlink precoding and equalization in satellite swarms," May 2022, submitted to *IEEE Transactions on Wireless Communications*. [Online]. Available: <https://arxiv.org/abs/2205.11180>

- [16] D. Tse and P. Viswanath, *Fundamentals of Wireless Communication*. Cambridge, U.K.: Cambridge Univ. Press, 2005.
- [17] C. Windpassinger, “Detection and precoding for multiple input multiple output channels,” Ph.D. dissertation, Friedrich-Alexander-Universität Erlangen-Nürnberg (FAU), 2004.
- [18] S. Chatzinotas, G. Zheng, and B. Ottersten, “Energy-efficient MMSE beamforming and power allocation in multibeam satellite systems,” in *2011 Conference Record of the Forty Fifth Asilomar Conference on Signals, Systems and Computers (ASILOMAR)*, 2011, pp. 1081–1085.